Korean Journal of Remote Sensing, Vol.19, No.1, 2003, pp.61~70

Automatic Identification of Fiducial Marks Based on Weak Constraints

Seong-Ik CHO and Kyoung-Ok KIM

Spatial Information Technology Center,
Electronics and Telecommunications Research Institute, Korea

Abstract : This paper proposes an autonomous approach to localize the center of fiducial marks included in aerial photographs without precise geometric information and human interactions. For this localization, we present a conceptual model based on two assumptions representing symmetric characteristics of fiducial area and fiducial mark. The model makes it possible to locate exact center of a fiducial mark by checking the symmetric characteristics of pixel value distribution around the mark. The proposed approach is composed of three steps: (a) determining the symmetric center of fiducial area, (b) finding the center of a fiducial mark with unit pixel accuracy, and finally (c) localizing the exact center up to sub-pixel accuracy. The symmetric center of the mark is calculated by successively applying three geometric filters: simplified $\nabla^2 G$ (Laplacian of Gaussian) filter, symmetry enhancement filter, and high pass filter. By introducing a self-diagnosis function based on the self-similarity measurement, a way of rejecting unreliable cases of center calculation is proposed, as well. The experiments were done with respect to 284 samples of fiducial marks composed of RMK- and RC-style ones extracted from 51 scanned aerial photographs. It was evaluated in the visual inspection that the proposed approach had resulted the erroneous identification with respect to only one mark. Although the proposed approach is based on weak constraints, being free from the exact geometric model of the fiducial marks, experimental results showed that the proposed approach is sufficiently robust and reliable.

Key Words : Fiducial Marks, Automatic Identification, Interior Orientation.

1. Introduction

Aerial photographs taken by an aerial camera are calibrated generally through the procedures of interior orientation, relative orientation, and absolute orientation before they are processed for extracting the precise geographic information of ground objects. Among them, the interior orientation is a process of establishing the transformation from pixel to photo coordinate. The location of the principal point, representing the geometric center of a photograph, is calculated from the location of fiducial marks that is typically located in four corners and/or four sides of the photograph, and is composed of several geometric primitives such as lines, circles and a point. Autonomous interior orientation for determining the exact center of a fiducial mark without

Received 23 December 2002; Accepted 25 January 2003.

human interaction can be a challenging issue in developing advanced digital photogrammetric workstations (Kölbl, 1996; Heipke, 1997; Schenk, 1999).

There have been several previous researches such as binary cross correlation, least-square template matching (Schenk, 1999), modified Hough transformation (Kersten and Haering, 1997), and attribute-based mathematical morphology (Sun and Wu, 2001). However, there have been restrictions such as the requirement of a priori knowledge about the precise geometric shape or the image database of the mark.

In our previous research (Cho *et al.*, 2001; Cho *et al.*, 2002), a new approach based on radiometric and geometric analysis of fiducial marks had been proposed. In those papers, a candidate region for a fiducial mark is isolated by applying binarization process and mathematical morphology, and then the center location is determined up to unit pixel accuracy by applying $\nabla^2 G$ (Laplacian of Gaussian) filtering and a symmetry enhancement filtering. The approach might be evaluated as a meaningful advance in the sense that it does not require exact geometric information of the mark. However, there are restrictions that it is applicable to the style of large-sized and complex-shaped fiducial marks only, and that the determination of exact center and the lack of self-diagnosis functions are remained as the open problems.

For compensating those restrictions inapplicable to various styles of fiducial marks, an advanced conceptual model concerning the fiducial area and the fiducial mark is proposed in this paper. Based on the conceptual model, a novel idea is proposed to precisely locate the sub-pixel center of a mark autonomously without relying on the detailed geometric model and human interactions.

Section 2 discusses the conceptual model and the strategy in analyzing the fiducial mark. Detailed approach in localizing the exact center of a fiducial mark is discussed in Section 3. Experimental results are shown in Section 4, and finally Section 5 concludes this paper.

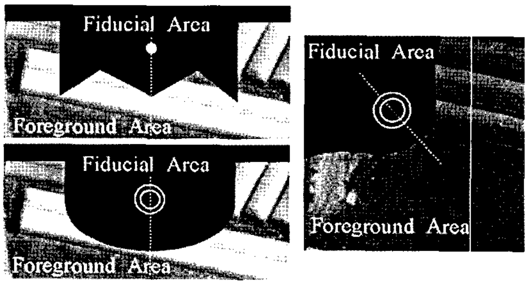

(a) Center area (b) Corner area

Fig. 1. Conceptual model of fiducial marks.

2. Conceptual Model and Strategy

1) Conceptual Model

The radiometric model proposed for isolating the fiducial mark from the fiducial area (Cho *et al.*, 2001; Cho *et al.*, 2002) has a restriction that the spatial extent of the mark is so large as to be distinguished and isolated in morphological filtering. This restriction makes it difficult to isolate a meaningful geometric pattern from the background when the mark is composed of the simple geometric primitives such as a dot or a tiny cross.

In order to overcome this restriction, we are proposing an advanced approach based on a generalized conceptual model of the fiducial area and the fiducial mark. The model is based on the following two assumptions:

① *The geometric characteristics of a fiducial mark is exactly symmetric with respect to any axis that passes the center of the mark,*

② *The fiducial area is roughly symmetric with respect to the axis that passes the center of the mark.*

Although the assumptions should be classified as *weak constraints* in the senses that they are not relying on the exact geometric model of the mark, they play a critical role in analyzing an image containing the mark. The important meaning of the assumption ① is that the geocentric center of the mark is exactly same with the symmetric center, constituting core of the proposed approach as the primary symmetric constraint.

Fig. 1 shows the simulated images of typical fiducial mark, fiducial area and foreground area, where dotted line appeared in the model means the symmetric axis of the fiducial area.

2) Strategy

The strategy for localizing the center of a fiducial mark is based on the above assumptions. The strategy is fundamentally based on the fact that the intersection of two perpendicular axes in two-dimensional space determines one point exactly. One axis passing center of the mark can be obtained by finding symmetric axis of the fiducial area because it is assumed, by the assumption ②, that the axis dividing that area symmetrically passes the center location of the mark. That is, the center location of the mark is determined by finding the axes L1, L2, L3, and L4 sequentially, as shown in Fig. 2. Where, L1 and L2 denote vertical limits of the fiducial area, L3 the symmetric axis of that area, L4 the symmetric axis of the mark being perpendicular to L3. When the mark at corner area is concerned, target image is diagonally projected before localizing the symmetric axis for lining up the axis in vertical direction.

Detailed procedure of localizing the center of the mark is shown in Fig. 3. After determining the upper (L1) and lower bound (L2), the symmetric axis of the area (L3) is determined. This procedure of the fiducial area analysis is supported by the assumption ②. The symmetric center of the mark is calculated and refined iteratively by sequentially applying the following operations: simplified $\nabla^2 G$ filtering, symmetry enhancement filtering, and high pass filtering.

This procedure of the fiducial mark analysis is

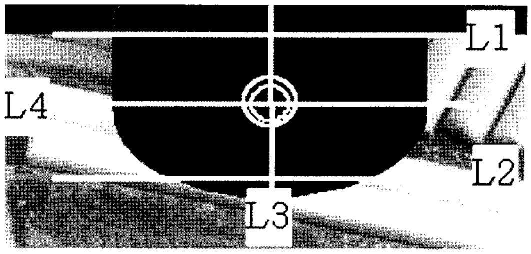

Fig. 2. Sequential order in finding the center location of a mark.

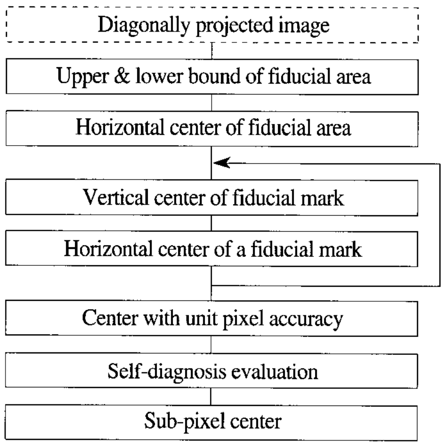

Fig. 3. Procedure of localizing the exact center of a fiducial mark.

supported by the assumption ①. After performing self-diagnosis evaluation, center location of the mark is determined with unit pixel accuracy. Finally, the location is precisely determined up to sub-pixel accuracy by using the enlarged image of the mark.

3. Identification of Fiducial Marks

1) Fiducial Area Analysis

The upper and lower bounds of the fiducial area, L1 and L2 as shown in Fig. 2, are determined by analyzing the accumulated profile of the vertical edge. This profile of input image *IO* is calculated by the following equation:

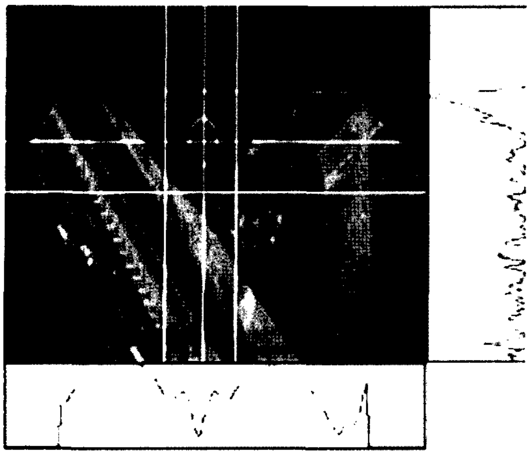

Fig. 4. Calculation of the center location of a RC-style fiducial mark.

$$I_v(y) = \sum_{x=p1}^{p2} |IO(x, y-d) - IO(x, y+d)|, \quad (1)$$

where, I_v denotes the resultant profile, d the pixel separation used for edge calculation, and $p1$ and $p2$ horizontal interval of accumulation. As shown in right side of Fig. 4, the location of upper bound is determined by finding the intersection between the accumulated profile and a given threshold value. In this paper, the average value of the profile is adopted as the threshold.

The horizontal extent of the fiducial area is calculated by analyzing and thresholding vertically accumulated profile of the input image. This accumulation is done with respect to the sub-image existing below the upper bound. In a similar way of determining the upper bound L1, the lower bound L2 can be determined by analyzing the profile accumulated within the range bounded by L1 and horizontal extent.

Finally, the symmetric center of the fiducial area L3 can be determined by analyzing the symmetric characteristics of a portion of image bounded by horizontal extent and by vertical limits L1 and L2. When I_a denotes vertically accumulated profile of the portion bounded by L1 and L2, the symmetric characteristics of that profile is calculated by the following equation:

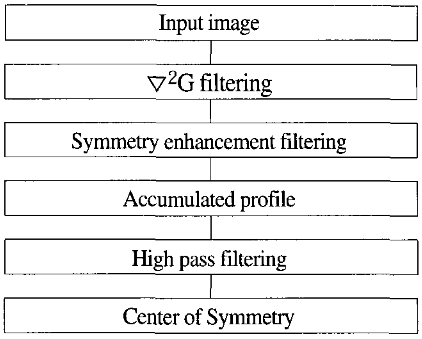

Fig. 5. Procedure of calculating the center of symmetry.

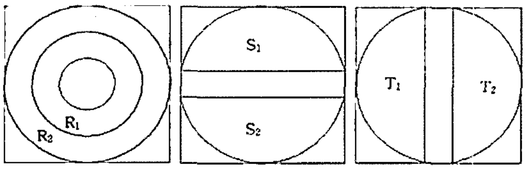

Fig. 6. Convolution kernel used for (a) G filtering, (b) vertical symmetry filtering, and (c) horizontal symmetry filtering.

$$I_s(x) = \sum_{u=1}^{d} |I_a(x+u) - I_a(x-u)|, \quad (2)$$

where, I_s denotes result of the symmetry calculation, d the interval of calculation. The symmetric center is determined by finding the minimum of the profile I_s, which is shown in the bottom side of Fig. 4.

Other style of the fiducial area, such as RMK-style one, can be processed in the same way. This procedure is autonomous because it is processed without human interaction.

2) Fiducial Mark Analysis

By applying the fiducial area analysis, the center of a fiducial mark is restricted to neighborhood of the line L3 by the assumption ②. The fiducial mark analysis determines center of the mark by calculating center of symmetry as shown in Fig. 5. This procedure starts by applying the ∇^2G filter for the enhancement of input image. Since this filtering generates zero crossings at the edge (Marr, 1982), the resultant image is sensitive to symmetry enhancement filtering as far as the window size of convolution kernel used for the filter is comparable to the size of target object. At next step, a symmetry enhancement filter is applied for determining the symmetric center of the mark, since the geometry of the mark is symmetric at the center by the assumption ①. Those filterers are applied with respect to certain area of interest (AOI) restricted by the neighborhood of L3 and vertical limits L1 and L2. Then, one-dimensional profile is produced by accumulating pixel values of AOI of the image generated by the symmetry enhancement filtering. It is accumulated vertically when horizontal center is concerned, and so horizontally for vertical one. This is because the purpose of accumulation is in enforcing symmetric information spread in pixels of AOI. Finally, the center of symmetry with unit pixel accuracy is determined by finding the peak of the profile generated by applying a high pass filtering into the accumulated profile.

A simplified $\nabla^2 G$ filtering, rather than the original $\nabla^2 G$ filtering, defined by the equation,

$$I2(x, y) = \frac{1}{N_{R2}} \sum_{(u,v)\in R2} IO(x+u, y+v) - \frac{1}{N_{R1}} \sum_{(u,v)\in R1} IO(x+u, y+v) \quad (3)$$

is implemented for the fast calculation. Where N_{R1} and N_{R2} denote the number of pixels of the regions $R1$ and $R2$ defined by the convolution kernel, as shown in Fig. 6(a). Equation (3) means difference of the average value of two regions $R1$ and $R2$. The filtering defined by equation (3) and is faster than the original $\nabla^2 G$ filtering because it supports the box-filtering technique (McDonald, 1981).

The symmetry enhancement filtering is efficient in enhancing symmetric information formulated by pixels composing an object having reflection symmetry (Cho *et al.*, 2002). This filtering in vertical and horizontal direction is defined by the following equations, respectively:

$$I3_h(x, y) = \sum_{(u,v)\in T1} |I2(x+u, y+v) - I2(x-u, y+v)|, \quad (4)$$

$$I3_v(x, y) = \sum_{(u,v)\in S1} |I2(x+u, y+v) - I2(x+u, y-v)|, \quad (5)$$

where $S1$ and $S2$ denote the region of vertically symmetric convolution kernel defined in Fig. 6(b), and $T1$ and $T2$ that of horizontally symmetric one defined in Fig. 6(c). Equation (4) means sum of the absolute difference of symmetrically located pixels in the regions $S1$ and $S2$, and equation (5) does in a similar way.

The accumulation of pixel value converts two-dimensional image into one-dimensional profile by the following equation:

$$I4_h(x) = \sum_{v=-d}^{d} I3_h(x, y+v), \quad (6)$$

where d denotes the interval of accumulation and $I4_h(x)$ horizontally accumulated profile.

High pass filtering is defined by the following equation:

$$I5_h(x) = \frac{1}{(2d+1)} \left[\sum_{u=-d}^{d} I4_h(x+u) \right] - I4_h(x), \quad (7)$$

where d denotes the interval of smoothing. This filter is adequate in finding the center of symmetry because it is sensitive to the steep variation of a given signal, and because the center of symmetry included in the accumulated profile satisfies the condition.

Fig. 7 shows the results of those filtering applied with respect to a sub-image containing RMK- and RC-style marks. Location of the peak generated by high pass filtering corresponds to the center of symmetry calculated in vertical direction. The center of symmetry coincides to the geometric center of the mark by the assumption. Therefore, the geometric center of a mark can be determined up to unit pixel accuracy by the proposed procedure of the fiducial mark analysis.

One of the important advantages of the proposed

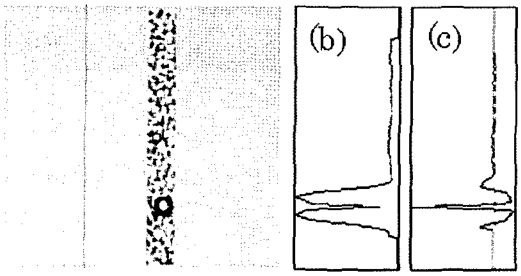

RMK-style finducial mark

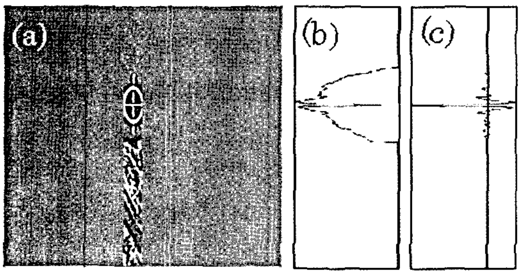

RC-style fiducial mark

Fig. 7. Calculated results of (a) ∇^2G filtering, (b) Symmetry enhancement filtering, and (c) High pass filtering.

approach is that it is free from the specific geometry of the mark because it determines the center by calculating just the symmetric characteristics of the mark. Another one is that all the parameters can be determined internally without human interaction. It is sufficient to fix the inner radius of $R1$ as two, outer one as three, and outer one of $R2$ as four in pixel unit because ∇^2G filtering is used for generating the zero crossing at the edge pixel. The radius of the convolution kernel of symmetry enhancement filtering should be set as large as the half-size of the target object. By analyzing the profile of target object, this radius can be stably determined because we are dealing with at least four marks having the same shape.

While the accumulation using wide range of interval results stable determination of center, in the calculation of equation (6) and equation (7), it generally results a little deviation. It is sufficient to fix the interval of accumulation defined in two equations as the half-size of the target object at first step of iteration. Then, the center location is refined iteratively, once in vertical direction and once in horizontal one, by narrowing the interval in the process of iteration. The iteration stops when iterative shift converges into one pixel or it diverges. When it diverges, the case is classified as the failure and all the process stops.

When relatively large mark such as RC-style one is concerned as shown in Fig. 8, the center position securely converges in the iteration even when initial deviation is not negligible. This is because the center of the mark indicated by the symmetry can be obtained stably even from a substantial part of the mark. In can be acknowledged from the figure that three substantial parts of the mark indicates almost the same location of the symmetric center.

3) Self-Diagnosis Evaluation

The self-diagnosis function used for checking the reliability of the calculated center is essential in developing an autonomous interior orientation process (Schenk, 1999; Sun and Wu, 2001). The self-similarity measure of the mark is adequate for evaluating reliability of the calculated center because it can be processed autonomously without external geometric model of the mark.

By assumption, there is little difference between the original sub-image of the mark and the self-symmetric addition of that as far as the center of the mark is determined correctly. However, two images become different when the calculation of the symmetric center has failed or when the object included in the sub-image

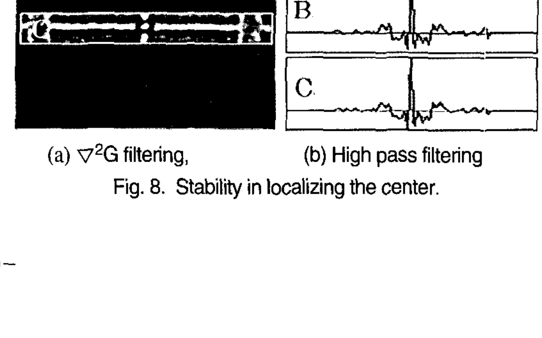

(a) ∇^2G filtering, (b) High pass filtering

Fig. 8. Stability in localizing the center.

is not symmetric in its geometry. The self-symmetric addition, in horizontal and vertical direction, is defined by the following equations, respectively:

$$S1(x, y) = I6(x, y) + I6(x_w - x, y), \tag{8}$$

$$S2(x, y) = I6(x, y) + I6(x, y_w - y), \tag{9}$$

where $I6(x, y)$ denotes the input sub-image, and $I6(x_w - x, y)$ and $I6(x, y_w - y)$ the symmetric images of $I6(x, y)$ reflected in horizontal and vertical direction. This addition has an advantage that it compensates local intensity variation of the mark, when correct center is obtained.

Again by assumption, there is little difference between the original sub-image and that rotated in 90 degrees as far as the axis of rotation is located at symmetric center of the mark. The rotation of the image $S1(u,v)$ is defined by the following equations:

$$S3(x, y) = Rot_{90}\{S1(u, v)\} \tag{10}$$

$$S4(x, y) = Rot_{90}\{S2(u, v)\} \tag{11}$$

where $Rot_{90}\{\ \}$ denotes rotation of the target image by 90 degrees at the center of image.

The self-diagnosis checking is evaluated by calculating the cross-correlation of two images; one is the image of self-symmetric addition and another is the rotated image of that. When $R\{S1, S2\}$ denotes the normalized cross-correlation of two images $S1$ and $S2$, the measure is defined by the following equation:

$$R12 = R\{S1, S2\}. \tag{12}$$

The measure for a sub-image containing a fiducial mark is evaluated by adding four possible combinations of the cross-correlation by the following equation:

$$R_{self} = \frac{R12 + R34 + R13 + R24}{4} \tag{13}$$

Since this measure is based on the normalized cross-correlation of self-similar images, R_{self} becomes close to 1.0 when correct center is obtained, whereas it is much less than 1.0 when incorrect center is obtained or when the target object is not symmetric in geometric senses.

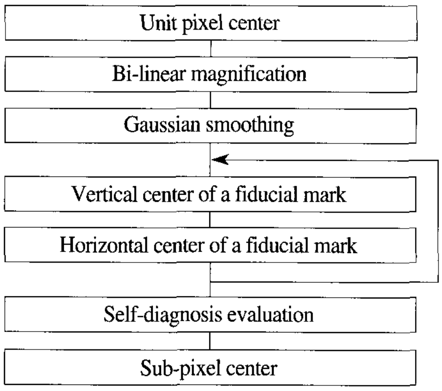

Fig. 9. Procedure of localizing the subpixel location of center.

The self-diagnosis measure should be used for evaluating whether the shape of target object satisfies assumption ① being the primary symmetric constraint of the conceptual model, and whether the center location obtained by the proposed approach is sufficiently reliable or not. Therefore, the self-similarity measure proposed in this paper is adequate for the self-diagnosis evaluation. When the value of R_{self} is lower than a given threshold, it is rejected and classified as the failure case. Adequate value of the threshold can be 0.5 as is usually adopted in similar procedure.

4) Sub-Pixel Location

It is necessary to determine the center of a fiducial mark up to sub-pixel accuracy, as possible, for the reliable performance of the interior orientation. The sub-pixel location is determined in a similar way of calculating the center with unit pixel accuracy, as shown in Fig. 9. A portion of image containing the neighborhood of the center pixel is extracted and enlarged by applying the bi-linear interpolation and the Gaussian smoothing filter. Location of the center in sub-pixel unit is calculated and refined iteratively by the same way of the fiducial mark analysis. Iteration stops when shift by iteration become less than one sub-pixel or when it diverges.

The location of sub-pixel center is determined by calculating the weighted mean location of center x_s defined by the following equation:

$$x_s = \frac{\sum_{x=-d}^{d} xI5(x)}{\sum_{x=-d}^{d} I5(x)}, \tag{14}$$

where $I5(x)$ denotes one-dimensional profile defined in equation (7), and d the interval of calculation. The interval is determined internally by calculating half of the extent where the value calculated by equation (7) is larger than zero in the neighborhood of the center.

Self-diagnosis measure is evaluated by using total shift of the sub-pixel center during the iteration process and by considering the standard deviation of pixel value in the neighborhood of the finally determined center. When total shift is larger than a given threshold or when the standard variation is smaller than a given threshold, it is classified as the failure case by regarding that the mark is too faint to be recognized.

Finally, the true center location of the mark is calculated by the following equation:

$$x_t = x_f + x'_p + \frac{x''_s}{R_e}, \tag{15}$$

where x_f denotes the center location of the sub-image within the original aerial photograph, x'_p the center of the mark measured relative to x'_f, x''_s the center location of the enlarged image measured relative to x'_p, and R_e the enlarged rate of the interpolation.

4. Experiments

Autonomous interior orientation starts from the layout analysis of scanned aerial photograph, which is not described in this paper, for extracting sub-images containing the fiducial area. The mark is identified and localized within each sub-image. The size of the sub-image containing the corner fiducial area was 1120 × 1120 in columns and rows and that containing the center fiducial area was 1120 × 700.

Experiments were done with respect to 284 sub-image samples containing the mark, as shown in table 1. Those samples are composed of 124 ones of RMK-style mark extracted from 31 photographs and 160 ones of RC-style mark done from 20 photographs. Computation was done on Pentium 1GHz with MS Windows 2000 environment. The manual evaluation for checking the reliability of the proposed approach is done in visual inspection with respect to each image.

In the visual inspection of total 284 samples, 247 samples were classified as the successful case localizing the center of the mark at least up to unit pixel accuracy. 36 samples were classified as the failure case, and one sample was done as the erroneous case. The failure case means that the sample was rejected by self-diagnosis function. The erroneous case means that it reported the wrong location of the center although it had not been rejected by self-diagnosis function. Three results of the successful case, where the sub-pixel location is estimated to be sufficiently reliable, are shown in Fig. 10. There was another style of the successful case having indistinct information about the accuracy of the sub-pixel location. Almost of the samples classified as the failure case, i.e. being rejected by the self-diagnosis function, were too faint to recognize the center location even in visual inspection. Fig. 11 shows the erroneous

Table 1. Experimental results.

style of the mark	No. of the sample	No. of the success	No. of the failure	No. of the erroneous	Processing Time (sec)
RMK	124	123	1	0	0.2
RC	160	124	35	1	0.6
Total	284	247	36	1	

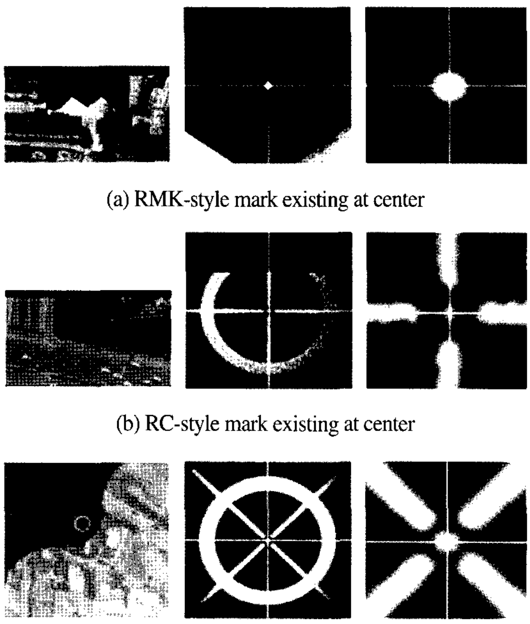

(a) RMK-style mark existing at center

(b) RC-style mark existing at center

(c) RC-style mark existing at centering

Fig. 10. Successful cases of centering.

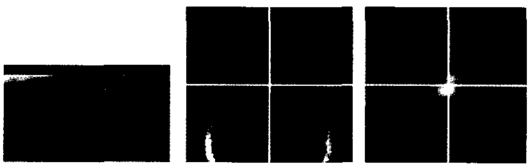

Fig. 11. Erroneous case.

case having reported the wrong location of the center.

The average processing time lapsed until the determination of the sub-pixel center was 0.2 second for RMK-style mark and 0.6 second for RC-style one, respectively.

5. Conclusions

We have proposed an approach in automatically identifying and localizing the exact center of the fiducial marks contained in scanned aerial photograph, with weak constraints not relying on the exact geometric model of the mark and free from human interactions. The conceptual model, established for defining and indicating the essential geometric characteristics of the mark, is composed of two assumptions concerning the geometric characteristics of general style of the fiducial area and the fiducial mark. The exact center location is determined by localizing it up to sub-pixel accuracy and by evaluating the self-diagnosis function designed for checking reliability of the calculation.

Experiments with respect to 284 samples of RMK- and RC-style marks showed that the only one results the wrong identification. Although 36 samples were rejected by self-diagnosis function, it does not mean the erroneous result of identification but the sound one because the function successfully rejected those cases that were hard to be identified even in visual inspection.

One of the important advantages of the proposed approach is that *it is autonomous* because it needs no specific geometric model, external parameters and human interactions. Another is that *it is robust and reliable* because it works well even when a part of the mark is chopped, and because it is based on the reliable self-diagnosis function.

References

Cho, S.I., C.H. Ahn, and Y.K. Yang, 2001. Automatic Identification of Fiducial Marks using Histogram and Geometric Analysis of Aerial Photographs, *Proc. of International Symposium on Remote Sensing,* Cheju, Korea, pp. 371-377.

Cho, S.I., K.I. Bang, and K.O. Kim, 2002. Automatic Identification of Fiducial Marks Existing in Aerial Photographs, *Journal of The Korean Society for Geo-Spatial Information System,* 10 (3): 79-87.

Heipke, C., 1997. Automation of Interior, Relative and Absolute orientation, *ISPRS Journal of Photogrammetry and Remote Sensing*, 52: 1-19.

Kersten T. and S. Haering, 1997. Automatic Interior

Orientation of Digital Aerial Images, *Photogrammetric Engineering and Remote Sensing*, 63 (8): 1007-1011.

Kölbl O., 1996. An Overview on Commercial Software Products for Digital Aerial Triangulation, *Proc. of OEEPE Workshop on Application of Digital Photogrammetric Workstations,* Lausanne, pp. 125-138.

Marr D., 1982. *Vision*, W.H. Freeman and Company, New York, USA.

McDonald, M. J., 1981. Box-Filtering Techniques, *Computer Graphics and Image Processing,* 17 (1): 65-70.

Schenk T., 1999. *Digital Photogrammetry,* Vol. 1, TerraScience, Ohio, USA.

Sun C. and X. Wu, 2001. Automatic Segmentation of Fiducial Marks Using Attribute-based Mathematical Morphology, *Journal of Electronic Imaging,* 10 (2): 560-566.